Redox Biology 17 (2018) 143–157

Contents lists available at ScienceDirect

Redox Biology

journal homepage: www.elsevier.com/locate/redox

Research Paper

Ameliorating mitochondrial dysfunction restores carbon ion-induced cognitive deficits via co-activation of NRF2 and PINK1 signaling pathway

Yang Liu[a,b,c], Jiawei Yan[a,b,c,d], Cao Sun[a,b,c], Guo Li[e], Sirui Li[e], Luwei Zhang[a,b,c], Cuixia Di[a,b,c], Lu Gan[a,b,c,d], Yupei Wang[a,b,c,d], Rong Zhou[a,b,c], Jing Si[a,b,c], Hong Zhang[a,b,c,*]

[a] Institute of Modern Physics, Chinese Academy of Sciences, Lanzhou 730000, China
[b] Key Laboratory of Heavy Ion Radiation Medicine of Chinese Academy of Sciences, Lanzhou 730000, China
[c] Key Laboratory of Heavy Ion Radiation Medicine of Gansu Province, Lanzhou 730000, China
[d] University of Chinese Academy of Sciences, Beijing 100039, China
[e] Lanzhou University, Lanzhou 730000, China

ARTICLE INFO

Keywords:
Carbon ions
Cognitive deficits
NRF2
PINK1
Mitochondrial dysfunction
Mitochondrial homeostasis
Redox balance

ABSTRACT

Carbon ion therapy is a promising modality in radiotherapy to treat tumors, however, a potential risk of induction of late normal tissue damage should still be investigated and protected. The aim of the present study was to explore the long-term cognitive deficits provoked by a high-linear energy transfer (high-LET) carbon ions in mice by targeting to hippocampus which plays a crucial role in memory and learning. Our data showed that, one month after 4 Gy carbon ion exposure, carbon ion irradiation conspicuously resulted in the impaired cognitive performance, neurodegeneration and neuronal cell death, as well as the reduced mitochondrial integrity, the disrupted activities of tricarboxylic acid cycle flux and electron transport chain, and the depressed antioxidant defense system, consequently leading to a decline of ATP production and persistent oxidative damage in the hippocampus region. Mechanistically, we demonstrated the disruptions of mitochondrial homeostasis and redox balance typically characterized by the disordered mitochondrial dynamics, mitophagy and glutathione redox couple, which is closely associated with the inhibitions of PINK1 and NRF2 signaling pathway as the key regulators of molecular responses in the context of neurotoxicity and neurodegenerative disorders. Most importantly, we found that administration with melatonin as a mitochondria-targeted antioxidant promoted the PINK1 accumulation on the mitochondrial membrane, and augmented the NRF2 accumulation and translocation. Moreover, melatonin pronouncedly enhanced the molecular interplay between NRF2 and PINK1. Furthermore, in the mouse hippocampal neuronal cells, overexpression of NRF2/PINK1 strikingly protected the hippocampal neurons from carbon ion-elicited toxic insults. Thus, these data suggest that alleviation of the sustained mitochondrial dysfunction and oxidative stress through co-modulation of NRF2 and PINK1 may be in charge of restoration of the cognitive impairments in a mouse model of high-LET carbon ion irradiation.

1. Introduction

In hadrontherapy, although high-LET carbon ions as an innovative modality of high-precision tool for the treatment of cancer, such as brain tumors and eye melanoma [1], potential damage to healthy tissues surrounding the tumor target along its penetrating path should still be considered. Given cancer therapy, there is a demand for reliable estimates of the effective protection of the normal brain against high-LET carbon ion radiation.

Brain has a high density of mitochondria, which are one of the main sources of reactive oxygen species (ROS), as it utilizes the oxygen for the energy production [2]. Overproduction of ROS results in the oxidative damage and mitochondrial dysfunction which have been implicated in the pathogenesis of several neurodegenerative diseases, including Alzheimer's disease, Parkinson's disease, Huntington's disease, Pelizaeus-Merzbacher disease and amyotrophic lateral sclerosis [3,4]. Recently, discoveries paint a rather cogent argument that mitochondrial positioning and shape can also affect the brain function and cognition [5,6]. Our previous data revealed that the ionizing radiation easily led to the mitochondrial ROS production, the alterations of the mitochondrial genome in the control region and the supercoiling formation of mitochondrial DNA as well as mitochondrial dysfunction which in turn enhanced ROS production [7–9]. Due to the lack of protective histones, limited DNA repair systems, mitochondria are more

* Corresponding author at: Institute of Modern Physics, Chinese Academy of Sciences, Lanzhou 730000, China.
E-mail address: zhangh@impcas.ac.cn (H. Zhang).

https://doi.org/10.1016/j.redox.2018.04.012
Received 7 February 2018; Received in revised form 13 April 2018; Accepted 13 April 2018
Available online 14 April 2018

vulnerable to oxidative damage and eventually to form a vicious cycle between mitochondrial dysfunction and oxidative stress [10].

PTEN-induced putative kinase1 (PINK1) encodes a highly conserved, 581-amino acid, putative serine-threonine protein kinase and conducts autophagic removal of damaged mitochondria through the modulation of mitochondrial network homeostasis and quality control [11,12]. Emerging data indicate that PINK1/Parkin system serves as key neuroprotective proteins in response to multiple stress conditions [13–15]. Particularly, several lines of evidence suggest that PINK1 protects cells from oxidative stress [16–18]. On the contrary, PINK1-deficient cells enhance susceptibility to oxidative stress as well [19,20].

Nuclear factor erythoid 2-related factor 2 (NRF2), a member of the cap 'n' collar subfamily of basic region-leucine zipper transcription factors, is an emerging regulator of the cellular expression of a number of genes to encode anti-oxidative enzymes, detoxifying factors, anti-apoptotic proteins and drug transporters [21,22]. NRF2 has been recently proposed as a therapeutic target for the treatment of neurodegenerative diseases, including Alzheimer's disease, Parkinson's disease, Amyotrophic lateral sclerosis, and Huntington's disease [23]. In addition, the emerging evidence of NRF2 has been found to modulate the mitochondrial function and metabolism [24,25].

Melatonin (N-acetyl-5-methoxytryptamine) is a powerful antioxidant that can easily permeate the blood-brain barrier and accumulate high concentration in mitochondria [26]. It is well demonstrated that melatonin has neuroprotective benefits for Alzheimer's disease [27], parkinsonism [28], aging [29], posttraumatic stress disorder [30], ischemic-stroke [31], neural tube defects [32], subarachnoid hemorrhage [33] and aging process [34]. There appears to be some evidence suggesting that the mechanism of neuroprotection of melatonin is partially mediated by the activation of NRF2 [35,36] or PINK1 [37,38]. In addition, melatonin had a marked inhibitory capacity on the developments of malignant brain tumors [39,40]. Intriguingly, the multiple actions of melatonin are known to vary between cancer and normal cells [41]. In doing so, if applicable to the clinical level, melatonin would have important implications in cancer therapies [42,43].

Hippocampus as one of the most vulnerable brain regions to oxidative damage is a brain region important for long-term memory and learning [44]. In this regard, herein this study has been undertaken to investigate the mechanisms of deterioration /amelioration of cognitive functions via modulating the key molecules of the signal transduction pathway in the hippocampus of the mouse brain after exposure to high-LET carbon ions.

2. Materials and methods

2.1. Animals

Male mice (26 ± 2 g) of outbred Kun-Ming strain obtained from Lanzhou Medical College (Lanzhou, China) were used. All animal studies were performed according to the requirements of the Animal Care Committee of the Institute. Mice were kept at a constant temperature (22 ± 1 °C) with a light-dark cycle (12 h light-12 h dark).

2.2. Cell culture

Immortalized mouse hippocampal neuronal cell line (HT22) obtained from BeNa Culture Collection (BNCC, Beijing, China). HT22 cell line were maintained in Eagle's minimum essential medium with non-essential amino acids (BNCC, Beijing, China), and supplemented with 10% (v/v) fetal bovine serum (Gibco, MA) and then incubated at 37 °C under 5% CO_2.

2.3. Irradiation procedure

The entire mouse and HT22 hippocampal cell line were irradiated with a high-LET carbon ion beams at the initial energy of 300 MeV u^{-1} generated from Heavy Ion Research Facility in Lanzhou (HIRFL, Institute of Modern Physics, Chinese Academy of Sciences, Lanzhou, China). Mouse and HT22 hippocampal cell line received a 4 Gy dose at a dose rate of about 0.5 Gy min^{-1}. The collimation of the beams to the place irradiated was controlled by a microcomputer. One month after 4 Gy carbon ion exposure, the hippocampal region of mouse brain were collected for the further experiments [45].

2.4. Morris water maze (MWM) test

Morris water maze (MWM) is a widely used behavioral test for evaluating neurocognitive ability of animal models [46]. MWM apparatus (ZS Dichuang New Technological Development Limited Liability Company, Beijing, China) which consist of a circular metal pool (120 cm in diameter, 40 cm in height, filled to a depth of 21 cm with water at 21 ± 1 °C) and a video capturing system were used to estimate the spatial learning and memory ability of mice. One month after carbon ion irradiation, during the experiment each mouse was given four trials per session for 5 days. They were placed in the water to find out the hidden platform to escape from the swimming. Each mouse has 120 s to find the hidden platform by itself; if the mouse failed to escape within this time, it was gently placed on the platform. Once the mouse reached the platform, it remained there for 10 s.

Five days after the acquisition phase, a probe test was conducted by removing the platform on the sixth day. The mice were allowed to swim freely in the pool. The time spent in the target quadrant, which had previously contained the hidden platform was recorded. The time spent in the target quadrant indicated the degree of memory consolidation, which had taken place after learning.

2.5. Histological study

Brain tissues which fixed in 4% paraformaldehyde were washed, dehydrated in ethanol with different concentration of 50–100%, cleared in xylene, and embedded in paraffin at 55 °C for 3 h. Paraffin blocks were cut with coronal sections by a microtome (Jung SM 2000R, Leica, Nussloch, Germany). Sections cut into 4 μm thickness were stained with H&E and Nissl (Beyotime Biotechnology, Nanjing, China). Sections were digitized using Pannoramic P250 Flash (3DHistech, Hungary).

2.6. Transmission electron microscope (TEM) observation

About 1 mm × 1 mm pieces were rapidly cut for brain, fixed in 4% formaldehyde and 1% glutaraldehyde in 0.1 M phosphate buffer (PH 7.4) for 2 h at room temperature and then post-fixed in 2.5% osmium tetroxide in 0.1 M phosphate buffer. After that, en bloc stain with 2% aqueous uranyl acetate for 1 h at room temperature in dark, dehydrated in graded ethanol and embedded in beam capsules. Sections, 70–80 nm-thick, were cut from the embedded tissue and collected onto grids to air dry overnight. Stained grids with uranyl acetate for 15–30 min and lead citrate for 3–15 min, and then observed under transmission electron microscope (JEM-1230).

2.7. Detection of respiratory chain complexes activities

The activities of mitochondrial respiratory chain complexes were performed as described previously [47]. After treatment with irradiation, cells were collected and washed twice with cold PBS. Cells were immediately pulverized by an ultrasonic cell Crusher (VCX130PB, SONICS Corporation). After determining the amount of total protein in the mixture, we detected the intracellular respiratory chain complex I (NADH dehydrogenase), complex II (succinic-coenzyme Q reductase), complex III (cytochrome c reductase), complex IV (cytochrome c oxidase) according to the instructions for reagent kits (Suzhou Comin Biotechnology, China).

2.8. ATP synthase activity measurement

ATP synthase activity was determined by a commercially available ATP synthase enzyme activity microplate assay kit (Abcam, Cambridge, MA) according to the manufacturer's instructions [48]. The change in absorbance at 340 nm between 12 and 30 min was recorded. The rate is calculated as ΔOD (m) /ΔT (min).

2.9. Detection of tricarboxylic acid (TCA) cycle enzymatic activities

Hippocampal cells were used for detecting the activities of pyruvate dehydrogenase (PDH), citrate synthase (CS), isocitrate dehydrogenase (ICDH), succinate dehydrogenase (SDH) and alpha-ketoglutarate dehydrogenase (α-KGDH) according to the manufacturer's instructions (Solarbio, Beijing, China) [49].

2.10. Intracellular ATP production

Intracellular ATP production measurement was performed using a commercially available luciferin-luciferase assay kit according to manufacturer's instructions (Beyotime Institute of Biotechnology, Shanghai, China) [50]. The bioluminescence value of mixture was measured with a microplate reader (Infinite M200, TECAN, and Switzerland).

2.11. Label-free Detection and Quantitation of Peptides

The peaklist of peptides was generated using DeCyder MS software version 1.0 (GE Healthcare, Piscataway, NJ) and the quantitative analysis of peptides was performed. Peptide detection, elution profile comparison, background subtraction and peptide quantitation were carried out on the full scan precursor massspectra in fully automatic mode. Peptide quantitation is based on MS signal intensities of individual LC-MS analyses. Different signal intensity maps were matched using the PepMatch module and then the peptide quantitative results were acquired. As there was no internal standard, the intensity distributions for all peptides detected in both samples were used for normalization. Throughout these studies the mass tolerance in the software was set to 0.5 amu and the retention time tolerance was set to 2 min.

2.12. Western blot analysis

The hippocampus of the brain was washed with PBS and then homogenized in 1 ml RIPA buffer with 100 μg/ml phenylmethylsulfonyl fluoride (Solarbio, Beijing, China) and further centrifugation at 12,000*g* for 20 min. The supernatant was collected, and the amount of protein was estimated by the BCA protein assay kit. Protein samples were loaded onto 10–12% sodium dodesyl sulfate (SDS) polyacrylamide gel, and then the proteins were transferred to polyethylene difluoride membranes (Millipore Corporation, USA). The membrane was blocked and subsequently incubated with anti-PINK1 antibody, anti-Parkin antibody, anti-superoxide dismutase 2 (SOD2) antibody and anti-NRF2 antibody (Abcam Inc, Cambridge, MA), anti-LC3B antibody (Genetex, Irvine, CA, USA), anti-dynaminrelated protein 1 (Drp1) antibody and anti-mitofusin 2 (Mfn2) antibody and anti-beta-actin antibody (Cell Signaling Technology, Inc., Beverly, MA, USA) for overnight at 4 °C. After primary antibody incubation was finished, the membranes were washed three times and incubated with HRP-conjugated secondary antibody. Secondary probes were detected by ECL Western blot detection reagents (GE Healthcare). The expression of protein was quantified using FluorChem FC2 software (Alpha Innotech Corporation).

2.13. Immunofluorescence analysis

In brief, these sections were de-paraffinized, immersed in citrate solution for antigen retrieval with an environment of high temperature and pressure, or proteinase K solution was added to the tissue and incubated for 5 min at 37 °C. And then the sections were treated with 0.2% Triton X-100 for 15 min at room temperature. Afterwards, sections were incubated with 1% bovine serum albumin (BSA) for 1 h and incubated with primary antibody to microtubule-associated proteins 1 A/1B light chain 3B (LC3B), PTEN-induced kinase 1 (PINK1), Translocase Of outer mitochondrial membrane 20 (TOMM20) and Cytochrome c oxidase subunit IV (COX IV, Abcam, Cambridge, MA) overnight at 4 °C. Then paraffin sections were exposed to Alexa Fluor-488 goat anti-mouse fluorochrome-conjugated secondary antibody and Alexa Fluor-555 goat anti-rabbit fluorochrome-conjugated secondary antibody (Invitrogen, Carlsbad, CA, USA) with the concentration of 0.2% in tris buffered saline (TBS) and maintained for 1 h in the dark. Slides were washed three times in PBS and medium containing 4′, 6-diamidino-2-phenylindole (DAPI) (Vector Laboratories, Burlingame, CA, USA). At last, expression and location of was observed using a laser scanning confocal microscope with a digital camera (LSM700, Carl Zeiss).

2.14. Determination of oxidative stress-related parameters

Mitochondria were isolated from the hippocampus of the mouse brain, according to instructions from a mitochondria isolation kit for tissue (Thermo Scientific, Rockford, USA). After that, analysis in levels of Malondialdehyde (MDA), 8-hydroxy-2′-deoxyguanosine (8-OHdG), total antioxidant capacity (TAC) and glutathione/oxidized glutathione (GSH/GSSG) ratio were performed using the commercial assay kits (Nanjing Jiancheng Bioengineering Institute, Nanjing, China, Shanghai Enzyme-linked Biotechnology, Shanghai, China) [51]. Microplate Reader was used for detecting (Infinite M200, TECAN, and Switzerland).

2.15. Flowsight data acquisition and analysis

Acquisition speed was set up to low speed and the highest resolution, an automated condition provided in Flowsight imaging flow cytometer (Amnis/Merck Millipore, Darmstadt, Germany) [52]. Approximately 5000 cells were acquired. Channel 5 was used to acquire DRAQ5 and channel 2 was used to detect Alexa Fluor 488. Data were analyzed in IDEAS software after compensation of single color control samples using a compensation matrix. The frequency of NRF2 translocation to the nuclei was analyzed using the nuclear translocation application wizard in IDEAS software.

Quantification of apoptotic cells was obtained using the Annexin V-FITC apoptosis detection kit (BD Biosciences, San Jose, CA, USA) according to the manufacturer's protocol. Following controls were used to set up compensation and quadrants: unstained cells and cells stained with FITC-Annexin V or with PI alone. The apoptotic/necrotic cell population was analyzed with a Flowsight imaging flow cytometer.

2.16. Protein/protein binding analysis

Co-immunoprecipitation (CO-IP) was performed for investigating the interactions of NRF2 and PINK1 according to the instruction from a Crosslink IP kit (Thermo Scientific, Rockford USA). 500 μg of protein in each group was incubated with 20 μl Protein A/G PLUS-Agarose for 30 min at 4 °C. After centrifugation at 1000*g* for 5 min at 4 °C, the supernatant was collected as the protein sample. Each protein sample was volume trice equally divided into 3 parts: IgG (negative control) Input (positive control) and CO-IP. Protein samples of CO-IP and IgG were respectively incubated with primary antibody and control IgG (Santa Cruz Biotechnology Inc) for 1 h at 4 °C, then, 20 μl of Protein A/G PLUS-Agarose was added, and the mixture was incubated on a rotating device overnight at 4 °C; after being centrifuged at 1000*g* for 5 min at 4 °C, immune-precipitates were collected and re-suspended in loading buffer for western blot analysis.

NRF2 and PINK1 binding analysis was performed using an OpenSPR localized surface plasmon resonance biosensor (Nicoya Life Science Inc., Kitchener, Canada). Firstly, we immobilized the NRF2 antibody at a concentration of 50 μg/ml on the activated COOH sensor chips using standard 1-ethyl-3-(3-dimethylpropyl)-carbodiimide plus N-hydroxysuccinimide, and then injected the blocking solution. 30 μg/ml total cell lysate protein was introduced into the sensor chip, and NRF2 was captured by the sensor. Finally, 50 μg/ml IgG as a negative control and PINK1 antibody as a target protein were injected into the sensor chip to detect the interaction with NRF2.

2.17. Transfection of HT22 cells

HT22 cells (5×10^4/well) were cultured in six-well plates until they grew to approximately 50% coverage, and were infected with the lentivirus. The following lentiviruses vectors were designed and constructed by Genechem (Genechem Company, Shanghai, China):

Lentiviruses vector, Ubi-MCS- − 3FLAG-SV40-EGFP-IRES-puromycin for NRF2 overexpression and Ubi-MCS-3FLAG-SV40-EGFP-IRES-puromycin for NRF2 negative control overexpression; lentiviruses vector, Ubi-MCS- − 3FLAG-CBh-gcGFP-IRES-puromycin for PINK1 overexpression and Ubi-MCS- − 3FLAG-CBh-gcGFP-IRES-puromycin for PINK1 negative control overexpression. After 12 h, the medium was replaced with fresh medium and were gathered cells for an additional 72 h.

2.18. Growth curve analysis

The rate of cellular proliferation was analyzed with an iCELLigence RTCA system (ACEA Bioscience, San Diego, CA, USA). Cells were grown on the surfaces of microelectronic sensors, which are composed of circle-online electrode arrays and are integrated into the bottom surfaces of the microtiter plate. Changes in cell number were monitored and quantified by detecting sensor electrical impedance. HT22 cells were harvested after different treatments and seeded into an E-8-well plate at a density of 5×10^3 cells/ well. The sensor devices were placed into the 5% CO_2 incubator and the cell index value was determined every hour automatically by the xCELLigence system for up to 72 h [53].

2.19. Statistical analysis

Data are presented as the mean ± standard error of the mean (SEM) from at least three independent experiment (n = 3). Two tailed *t*-tests were performed for single comparisons. Analysis of variance (ANOVA) was used for statistical comparison between different groups. If the p-value is under 0.05, the result is considered statistically significant.

3. Results

3.1. Cognitive deficits were induced by high-LET carbon ion irradiation

Morris water maze is the most common test used to assess cognitive function [46]. Morris water maze data on the platform for 6 consecutive days were represented in Fig. 1a-c to identify the degree of cognitive deficits induced by carbon ions. It can be observed that the escape latencies of the carbon ion radiation group showed conspicuous increases compared to the control group from day 2 to day 6 (Fig. 1b). On day 6, the mean escape latency of the control group, which decreased significantly compared to that on day 1, was found to be about 18 s. But in the irradiated group, it was found to be about 55 s. In the meantime, at sixth day, the residence time in the target quadrant through the virtual platform showed a significant reduction in the radiation group in contrast to in the control group (Fig. 1c). However, there were no effects on swimming velocity of all test animals.

The hippocampus is the key brain area for spatial learning and memory [54]. As seen in Fig. 1d-e, the morphological analysis focused on the hippocampus and serial sections with H&E staining revealed that the extent of the decrease and loose arrangement as well as the blurred caryotheca and pyknotic nuclei occurred in the hippocampus of the irradiated groups (Fig. 1e). Moreover, the group with carbon ion exposure showed a conspicuous reduction in the density of Nissl-stained cells in the hippocampal CA1 pyramidal neurons and granule cells of the dentate gyrus (DG). Notably, Nissl-stained dark neurons (N-DNs) with massive shrinkage and abnormal basophilia were observed in the irradiated DG including subgranular zone and granular layer as one kind of feature of damaged neurons (Fig. 1f). Cumulatively, these observations suggest that the high-LET carbon ion irradiation remarkably caused the hippocampus cognitive deficits, accompanied with the neurodegeneration and neuronal cell damage/death.

3.2. Mitochondrial damage was induced by carbon ions in the hippocampus region

As exhibited in Fig. 2a, electron micrographs showed that the mitochondria were swollen like empty bubbles, and the cristas broken and reduced, and the internal membranes fragmented in the irradiated mice. With regard to mitochondrial function, the results indicated that, after carbon ion exposure, the activities of mitochondrial respiratory chain complex I, IV and V (ATPase activity) in the hippocampus were prominently decreased by approximately 47.0%, 36.1% and 31.3% reduction compared with the control group, respectively (Fig. 2b), whereas compared with control mice, no significant difference in the activities of mitochondrial respiratory chain complex II and III was observed in the irradiated mice (data not shown).

Meanwhile, Pyruvate dehydrogenase (PDH) and tricarboxylic acid (TCA) cycle enzyme citrate synthase (CS), succinate dehydrogenase (SDH) and Alpha-ketoglutarate dehydrogenase (α-KGDH) in the irradiated mice all significantly declined in contrast to the sham-irradiated mice (Fig. 2c-d). To characterize the change of the energy metabolism evoked by carbon ions, ATP production was assayed in the irradiated hippocampal mitochondria. As a result, in the carbon ion irradiation group, there was about 29.1% reduction of ATP content of the control group (Fig. 2e). Collectively, these data imply that high-LET carbon ions caused the persistent impairments to mitochondrial structure and function at 1 month after irradiation.

Due to the dramatic changes taken place in the hippocampus, we used proteomics profiling to identify changes in protein expression that occur in the hippocampal cells at 1 month after irradiation with a dose of 4 Gy. In comparison with the control group, a total of 838 proteins (63 of which located in the mitochondria) was derived from LC-MS/MS analysis. The proteomics data were further analyzed by Gene Ontology, which included Biological Process (BP, Fig. 2f), Cellular Component (CC, Fig. 2g) and Molecular Function (MF, Fig. 2h). Focusing on BP linked to the mitochondrial function, two notable aspects were classified as shown in Fig. 2i: 1) bioenergetic process; 2) oxidative stress.

3.3. Carbon ions regulated the mitochondrial homeostasis in the hippocampus with or without melatonin

Considering in the significant alterations of the bioenergetic profiles and oxidative stress in the irradiated hippocampus, we investigated the underlying mechanisms of alleviation of hippocampal damage elicited by carbon ions through administration of melatonin (10 mg/kg daily for 7days i.p.) as a mitochondria-targeted antioxidant and a stabilizer of mitochondrial function [42]. Our data showed that carbon ions significantly increased Drp-1 (a major executor of mitochondrial fission) and decreased Mfn-2 (a key factor of mitochondrial fusion) in comparison with the control group. However, melatonin supplement prominently increased the expression of Mfn-2 1.6-fold and depressed Drp-1 by about 35.6% compared with the irradiation group, respectively (Fig. 3a-b).

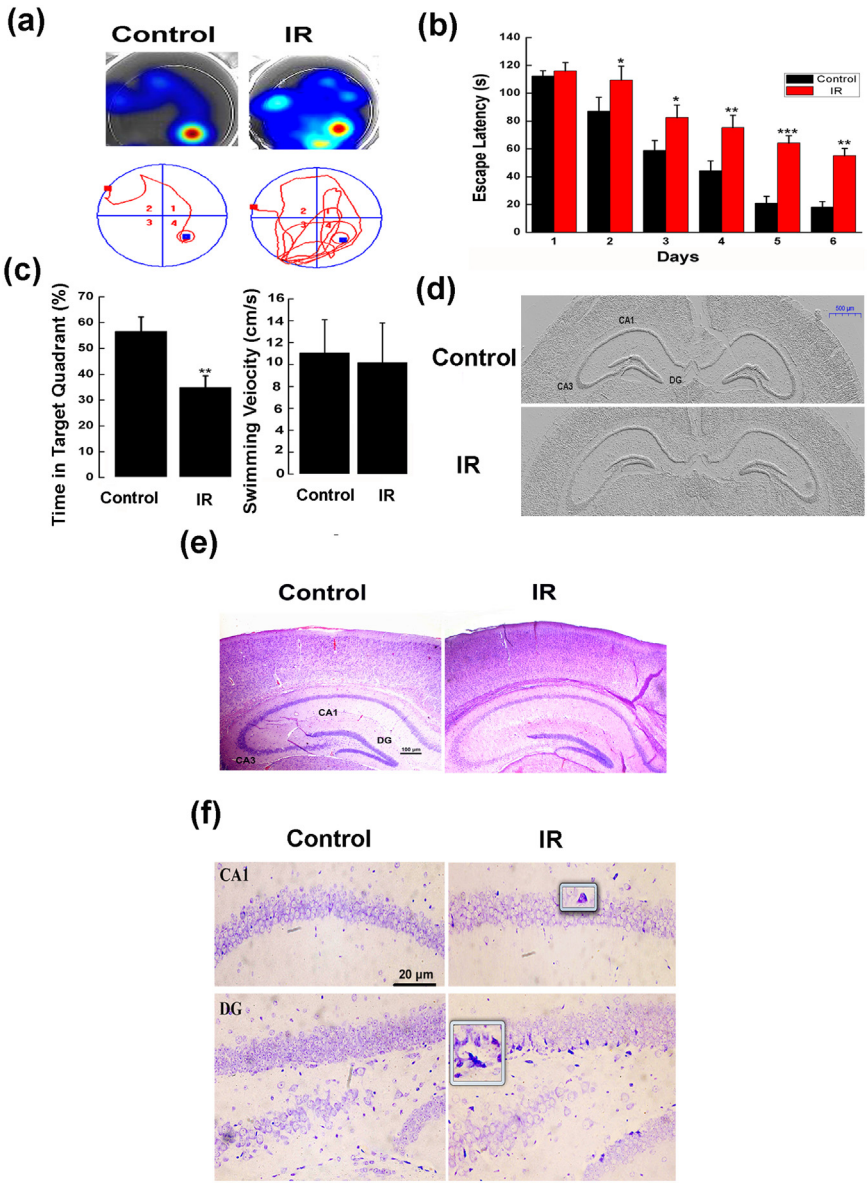

Fig. 1. Carbon ion irradiation caused the cognitive deficits (n = 6). (a) Representative heat map and tracing images of the test trials were evaluated for spatial learning and memory. (b) Escape latency in the irradiated group of on days 1–6 was conspicuously detected. (c) Swimming speed and time spent in the target quadrant was exhibited in the all groups. (d) Hippocampus structures of brain were scanned at 30 days after exposure to carbon ions. (e) H&E-stained hippocampus of mice was observed at 30 days after exposure to carbon ions. (f) Nissl-stained hippocampus of mice was observed at 30 days after exposure to carbon ions. Magnified views (white box) show Nissl-stained dark neurons. Values are presented as mean ± SEM. $^{*}P < 0.05$, $^{**}P < 0.01$, $^{***}P < 0.001$ versus the control group.

To determine whether carbon ion treatment regulated the mitophagy, we examined the quantity of mito-LC3 II in the irradiated hippocampus with or without melatonin. The analysis demonstrated that there was a notable observation of the decreased ratio of LC3II /LC3I in the irradiation group (Fig. 3c-d). On the other hand, co-location of LC3 and COX IV was considered to be an evidence for mitophagosomes as observed by confocal microscopy. In the carbon ion irradiated group, images showed that less obvious co-localization of COX IV (green) with LC3B (red)-positive signal was distributed in the cells (Fig. 3e). However, supplementation with melatonin dramatically restored the suppressive mitophagic process in the carbon-ion irradiated cells.

3.4. Carbon ions modulated the redox status in the irradiated hippocampus in the presence or absence of melatonin

Biomarkers of oxidative lesions can be quantitatively estimated with malondialdehyde (MDA) and 8-hydroxy-2′-deoxyguanosine (8-OHdG) in the brain hippocampus (Fig. 4a-b). Carbon ion group resulted in a significant augment in MDA level or 8-OHdG content related to the control group, indicating that carbon ions caused the chronic elevation in oxidative damage in the hippocampus. As expected, in comparison with the carbon ion group, our results showed that the greater reductions in the contents of MDA ($P < 0.01$) and 8-OHdG ($P < 0.01$) were observed in the irradiated animals with melatonin pretreatment.

For the anti-oxidative systems, our data exhibited that the TAC activity was reduced by about 37.3% in the irradiated group than in the control group (Fig. 4c). Moreover, Western blot results showed that the depressed expression of SOD2 was displayed in the irradiation-alone group (Fig. 4d), which plays an essential role in maintaining normal mitochondrial redox homeostasis, critical for the survival of eukaryotic cells. Additionally, the GSH/GSSG ratio was used to evaluate the cellular redox potential as shown in Fig. 4e. Compared with the control group, the carbon ion treatment caused a significant decrease in the GSH/GSSG ratio ($P < 0.05$). But pretreatment with melatonin markedly increased the TAC activity and the levels of SOD2 or GSH/GSSG.

3.5. Carbon ions regulated the PINK1 signaling pathway in the irradiated hippocampus with or without melatonin

The Pink1/Parkin system acts as a sensor for mitochondrial quality and modulated the mitophagy process [15,55]. Hence, we investigated the role of carbon ions in regulating PINK1/Parkin signaling pathway

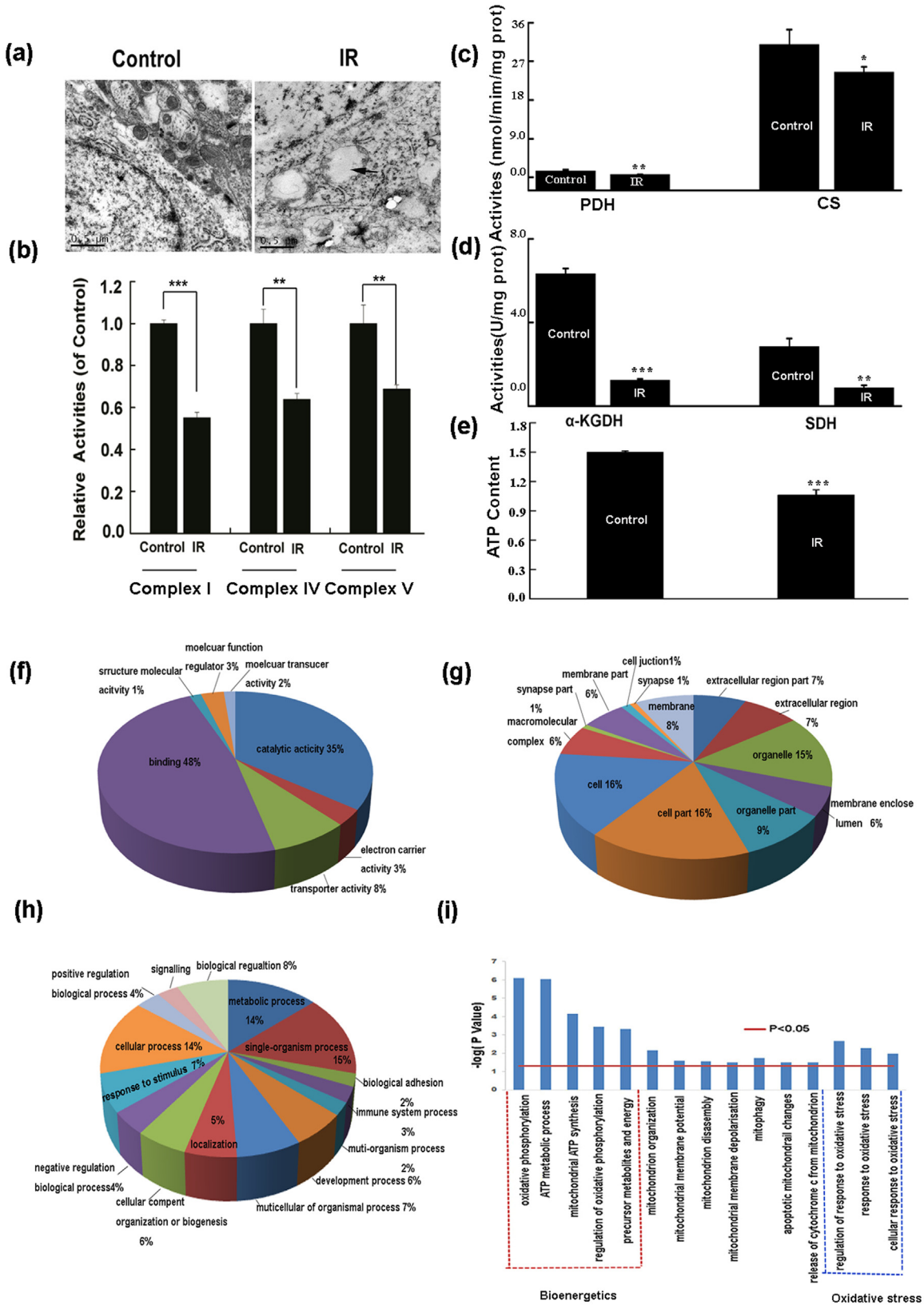

Fig. 2. Carbon ion irradiation induced the mitochondrial damage (n = 6). (a) Mitochondrial ultrastructural morphology was evaluated by transmission electron microscope. Black arrow indicates swollen mitochondria. (b) Enzymatic activities of mitochondrial respiratory chain enzymes were detected in the irradiated hippocampus. (c-d) Activities of TCA cycle enzymes and pyruvate dehydrogenate were measured in the irradiated hippocampus. (e) ATP content was detected in the hippocampus cells using the luciferin-luciferase assay. (f) Biological process using GO enrichment analysis. (g) Cell component using GO enrichment analysis. (h) Molecular function using GO enrichment analysis. (i) Significantly enriched biological processes were analyzed from proteomics data. Values are presented as mean ± SEM. $^{*}P < 0.05$, $^{**}P < 0.01$, $^{***}P < 0.001$ versus the control group.

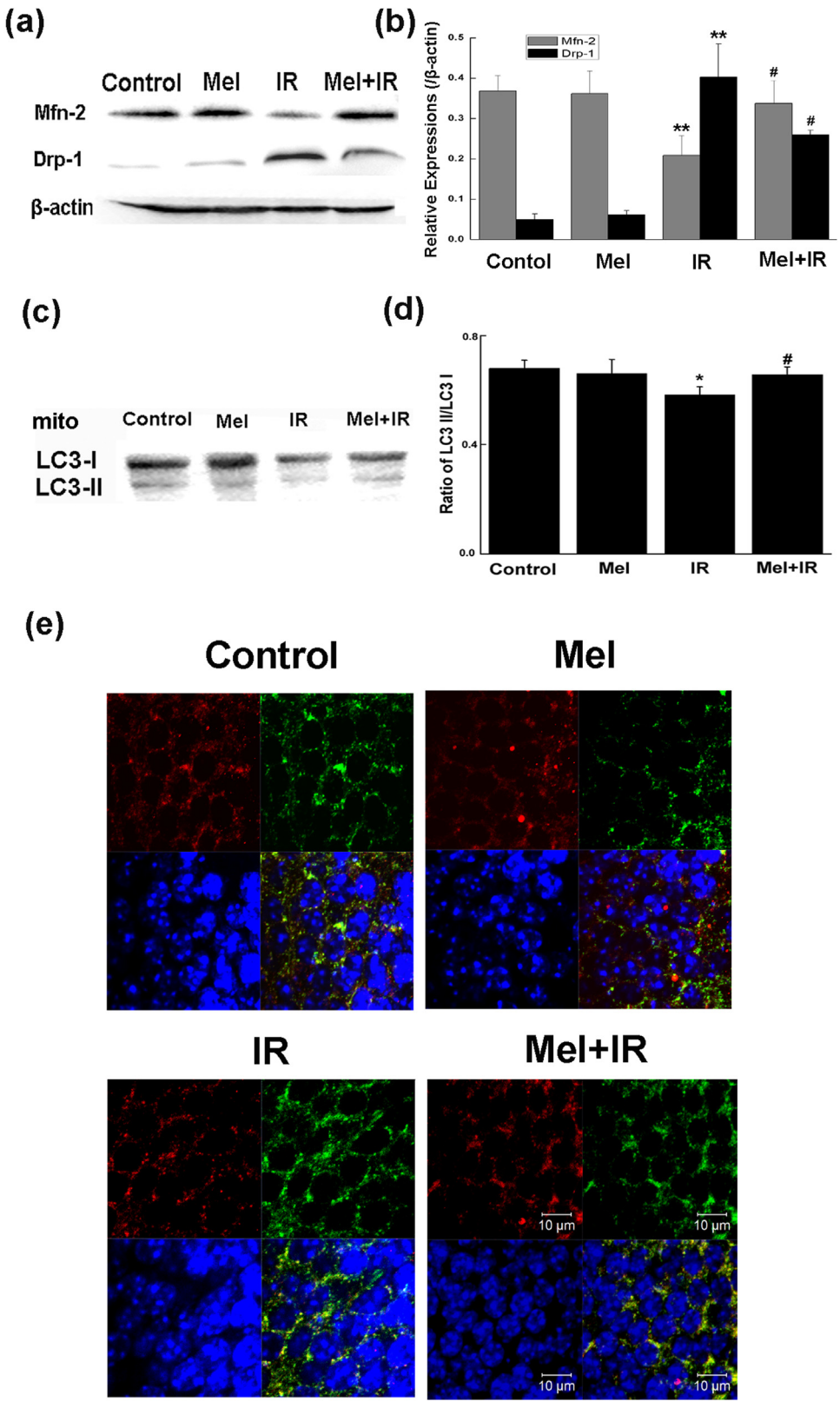

Fig. 3. Effects of carbon ions on the mitochondrial homeostasis-related proteins in the hippocampus of 1 month postirradiation with or without melatonin (n = 6). (a) Representative Western blots of Mfn-2 and Drp-1 were observed in the irradiated hippocampal cells with or without melatonin. (b) Quantitative data of Mfn-2 and Drp-1 were normalized by β-actin. (c) A representative Western blot of mito-LC3 was observed in the irradiated hippocampal cells in the presence or absence of melatonin. (d) Quantitative data of LC3 II normalized against LC3 I. (e) Co-localization of LC3 (*red*) and COX IV (*green*) was detected by confocal microscopy. Nuclei were counterstained with DAPI (*blue*). Values are presented as mean ± SEM. $^{*}P < 0.05$, $^{**}P < 0.01$ versus the control group; $^{\#}P < 0.05$ versus the irradiated group.

with or without melatonin. Confocal microscopy images as indicated in Fig. 5a revealed a weak PINK1 fluorescence in the DG region of the irradiated group in comparison to that of the control group. Moreover, in cells exposed to carbon ions, there was a marked decrease in the PINK1 and TOMM20 colocalization, indicating that carbon ions abated the PINK1 accumulation on the outer mitochondrial membrane. Quantitative data showed that the level of PINK1was markedly (about 36.3%) less in the radiation group than in the shamed irradiation group (Fig. 5b-c). But adding melatonin was obviously reversed these decreases. Likewise, the level of Parkin protein expression was substantially declined by irradiation, but melatonin pretreatment also restored this reduction.

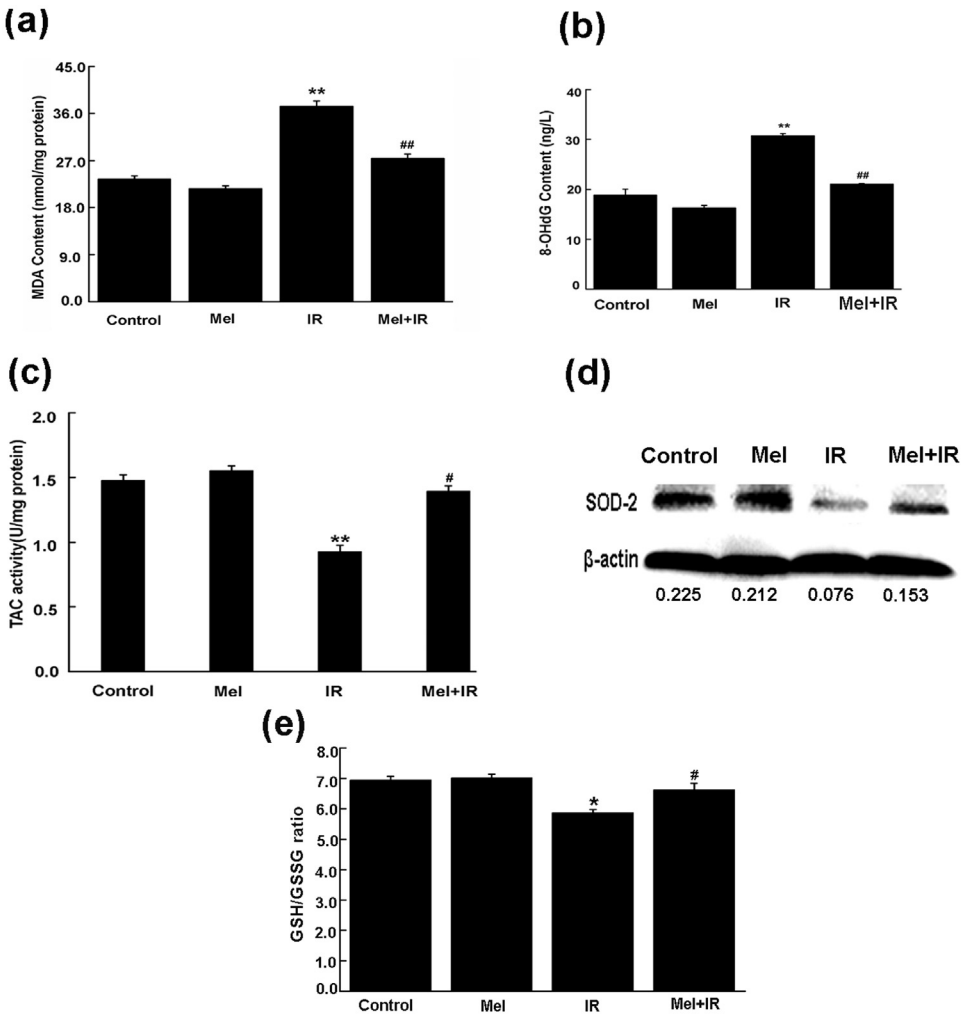

Fig. 4. The effects of carbon ion irradiation on redox systems were exhibited in the in the presence or absence of melatonin (n = 6). (a-b) MDA and 8-OHdG were detected as the hallmark of oxidative stress. (c) TAC enzyme was measured in the hippocampus to monitor the total antioxidant power. (d) Immunoboltting assay for SOD2 expression represented the mitochondrial antioxidant was measured in the irradiated hippocampus with or without melatonin. (e) The GSH/GSSG ratio was measured as an index of the redox status. Values are presented as mean ± SEM. $^{*}P < 0.05$, $^{**}P < 0.01$ versus the control group; $^{\#}P < 0.05$, $^{\#\#}P < 0.01$versus the irradiated group.

Altogether, our results indicated that carbon ions inhibited the PINK1/Parkin activation, whereas administration of melatonin could facilitate PINK1/Parkin activation in hippocampus cells, which are tightly related to the impaired mitochondrial homeostasis under high-LET carbon ion exposure.

3.6. Carbon ions modulated the NRF2 redox signaling in the irradiated hippocampus with or without melatonin

NRF2 is a transcription factor that responds to oxidative stress by binding to the antioxidant response element (ARE) [56]. Respected to the control group, there was no significant increment in the carbon ion irradiated group. Whereas, the level of NRF2 expression in the combined melatonin-radiation group was approximately increased 1.45-fold than that of in the irradiated group, while the opposite trend of expression of Keap1 was observed in Fig. 6a-b.

Furthermore, the data from Imaging Flow Cytometry showed that green color denoted NRF2 protein and red color denoted nucleus as observed in Fig. 6c. The merged color regions with high density represented the NRF2 translocation into the nucleus. Herein, there were lots of the merged color regions with low density in the carbon ion irradiated cells. Nonetheless, co-treatment with melatonin promoted the NRF2 nuclear translocation in the irradiated cells. Summarily, these data indicate that the reduced expression and translocation to the nucleus of NRF2 were mainly in charge of the imbalance of redox status caused by carbon ions.

Interestingly, as noted in Fig. 6e-g, our data demonstrated that significant co-immunoprecipitation of NFR2 with PINK1 and amplification of their binding signal were occurred in the cells treated with melatonin prior to the carbon ion irradiation using Co-IP and SPR assay. This evidence revealed that melatonin administration resulted in the positive interaction between NRF2 and PINK1 signaling.

3.7. Amelioration of cognitive deficits induced by carbon ions via regulating mitochondrial function

As seen in Fig. 7a, the results indicated that the decreased activities of PDH and TCA cycle CS, SDH and α-KGDH induced by carbon ion radiation were neutralized in the melatonin plus carbon ion treated group ($P < 0.01$, $P < 0.05$, $P < 0.001$ and $P < 0.001$). Meanwhile, our data showed that the activities of mitochondrial respiratory chain complex I and IV were prominently increased by approximately 1.6-fold and 1.3-fold in the hippocampus subjected to melatonin treatment prior to the carbon ions compared to the hippocampus irradiated with carbon ions alone, respectively (Fig. 7b). As a result, melatonin co-treatment prominently helped in the recovery of depressed ATP production induced by carbon ions (Fig. 7c). As observed in Fig. 7d, the escape latencies of the combination melatonin and carbon ion treatment group showed a significant decrease compared to the carbon ion exposed group.

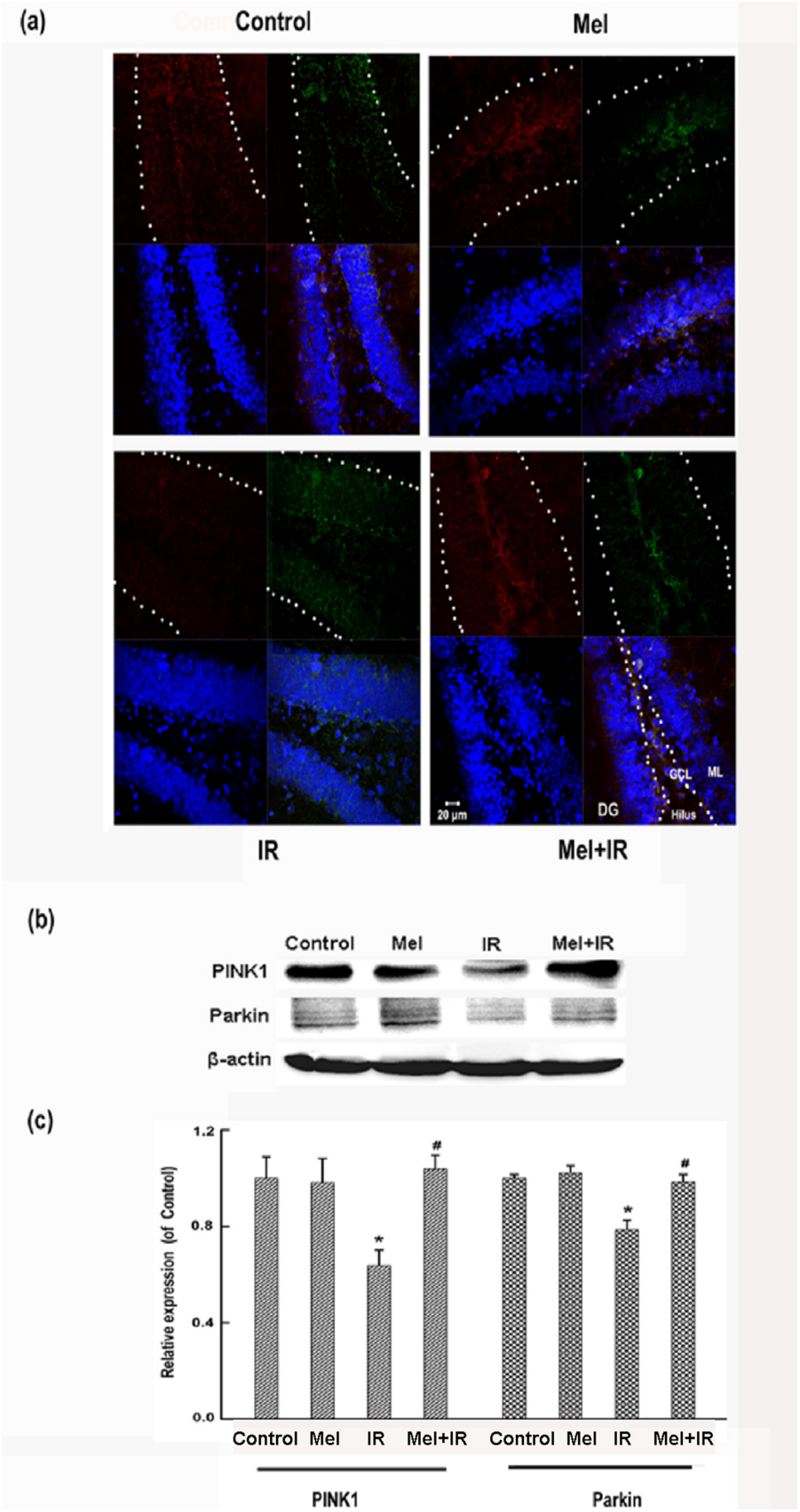

Fig. 5. Carbon ions modulated the PINK1-dependent pathway in the brain hippocampus pretreated with melatonin (n = 6). (a) Co-localization of PINK1 *(red)* and TOMM20 (*green*) was detected by confocal microscopy in the dentate gyrus at 1 month after irradiation with and without melatonin pretreatment. Nuclei were counterstained with DAPI (*blue*). (b) Western blot analysis for PINK1 and Parkin was performed on whole extracts of the hippocampus. (c) Quantifications of average western blot ban intensity are mean ± SEM. $^{*}P < 0.05$ versus the control group; $^{\#}P < 0.05$ versus the irradiated group.

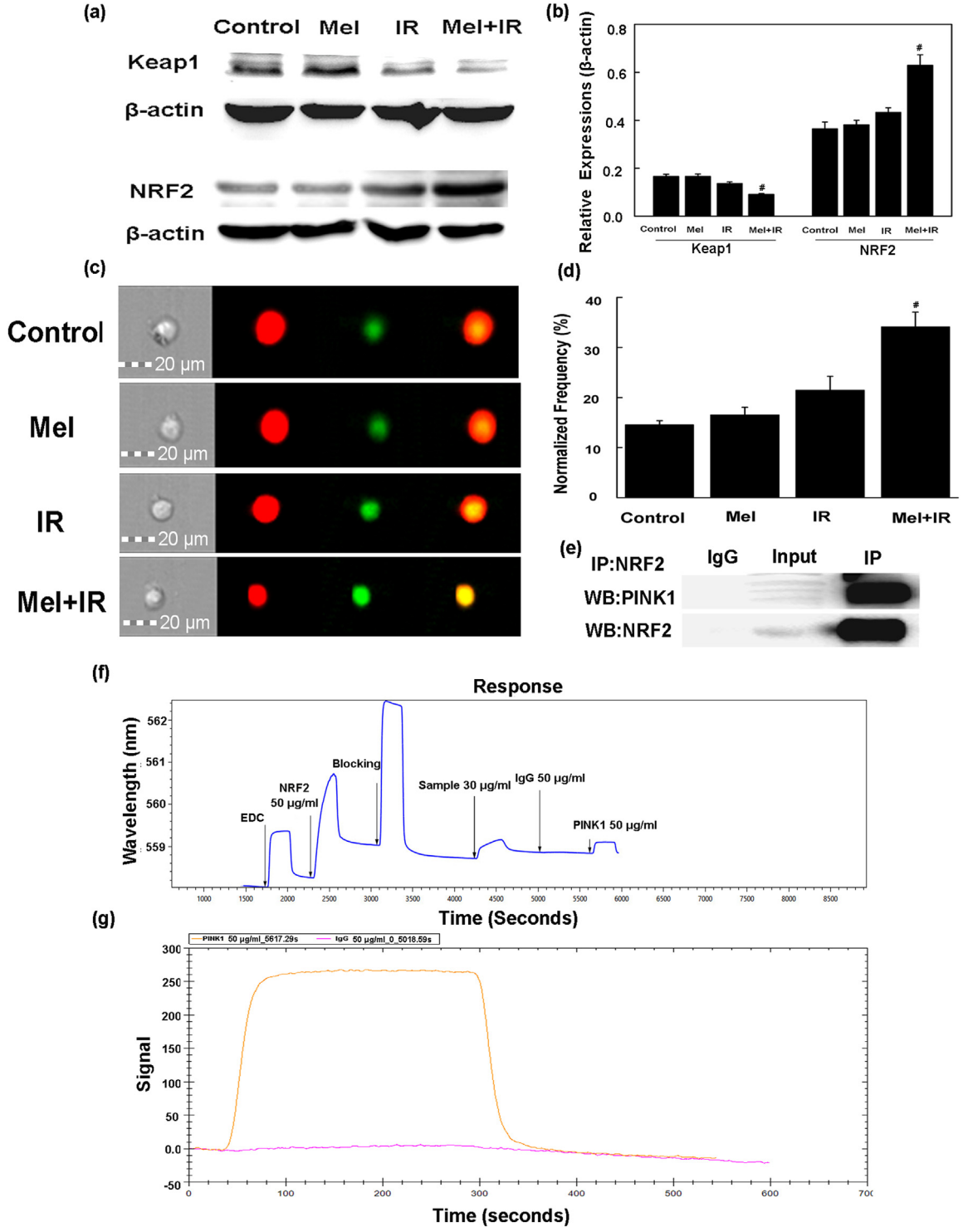

Fig. 6. Carbon ion irradiation modulated the redox signaling NRF2 in the brain hippocampus pretreated with melatonin (n = 6). (a) Immunoblotting assay for Keap1 and NRF2 expression was measured. (b) Quantifications of average western blot ban intensity were represented as mean ± SEM. (c) NRF2 nuclear translocation was detected in the cells using Flowsight. Green color demotes NRF2 protein and red color indicates the nucleus. (d) The nuclear translocation frequency of NRF2 protein was calculated. (e) Co-IP with NRF2 antibody followed by immunoblot with PINK1 primary was performed in hippocampus exposed to carbon ions with melatonin pretreatment. (f-g) NRF2/PINK1 binding analysis was performed using an OpenSPR assay. Yellow curve denotes the signal of PINK1 and Pink curve denotes the signal of the negative control. Values are presented as mean ± SEM. $^{\#}P < 0.05$ versus the irradiated group.

3.8. Neuroprotection against the injury induced by carbon ions via NRF2 and PINK1 signaling pathway

To better understand the cellular mechanisms of neuronal injury and protection, the expression levels of NRF2 and PINK1 were dramatically increased by lentiviral vectors in the mouse hippocampal neuronal cell line (HT22) (Fig. S3). As seen in Fig. 8a, compared to the sham-irradiated cells, carbon ion irradiation significantly inhibited the growth of HT22 cells for up to 72 h, and increased obvious proportion of apoptotic cells at 48 h after exposure to carbon ions (Fig. 8b). This

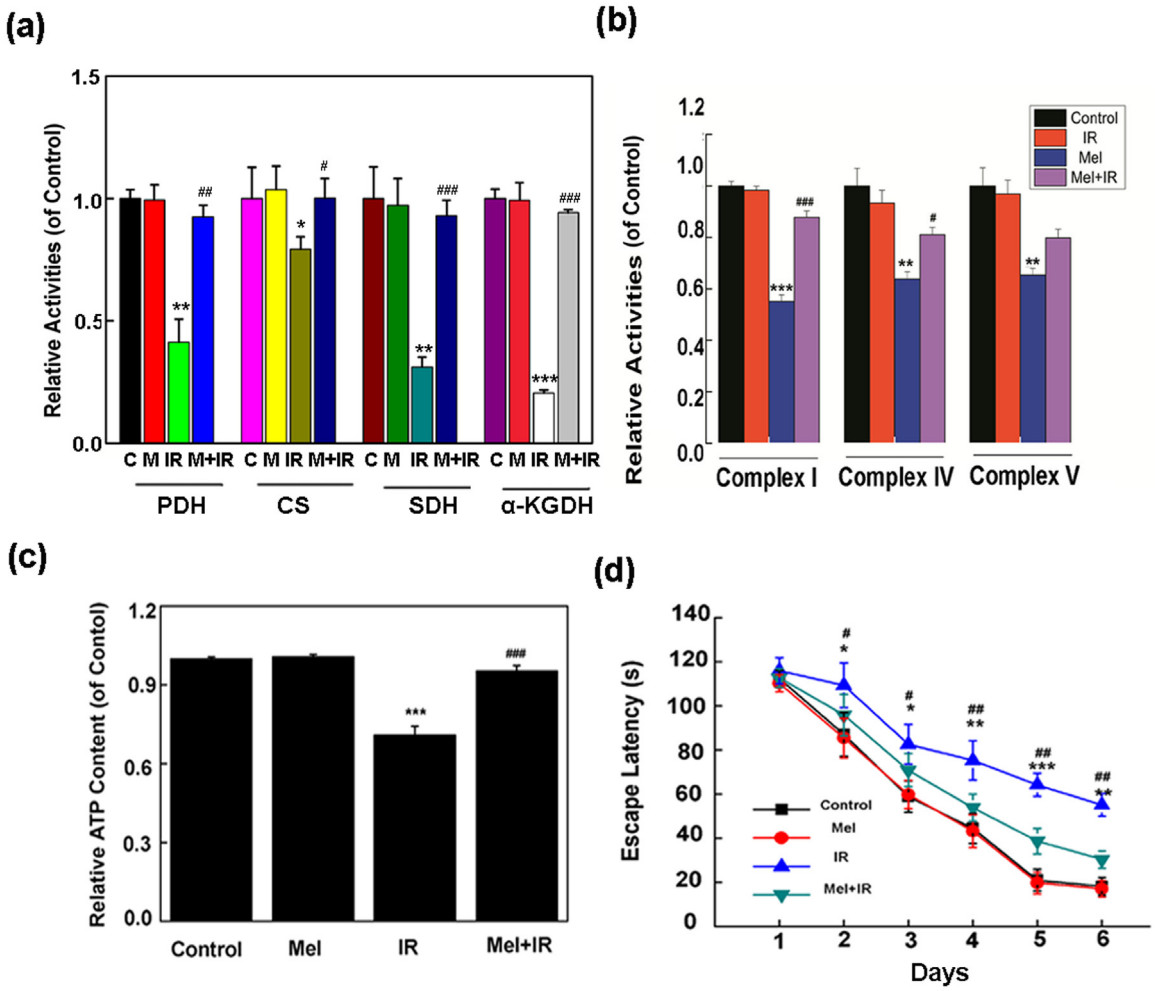

Fig. 7. Regulation of mitochondrial function ameliorated carbon ion-induced cognitive deficits (n = 6). (a) Activities of TCA cycle enzymes and pyruvate dehydrogenate were measured in the irradiated hippocampus with melatonin administration. (b) Enzymatic activities of mitochondrial respiratory chain enzymes were detected in the irradiated hippocampus with melatonin administration. (c) ATP content was detected in the hippocampus cells in the presence of melatonin. (d) Escape latency in the test groups of on days 1–6 was conspicuously detected. Values are presented as mean ± SEM. $^{*}P < 0.05$, $^{**}P < 0.01$, $^{***}P < 0.001$ versus the control group; $^{\#}P < 0.05$, $^{\#\#}P < 0.01$, $^{\#\#}P < 0.01$versus the irradiated group.

observation demonstrated that the inhibition of proliferation might be an apoptosis-dependent induction in the irradiated hippocampal cells. However, overexpressions of NRF2 and PINK1 notably restored the cell growth, and prominently decreased the number of apoptotic cells in the hippocampal cells treated with carbon ions.

4. Discussion

Owing to a focused dose distribution in addition to high-LET and subsequently high relative biological effect, carbon ion radiotherapy in cancer treatment is growing rapidly [57,58]. However, compared to low-LET ionizing irradiation, high-LET carbon ions, also produce more cytotoxic and genotoxic to normal cells [59]. The brain with highly peroxidizable fatty acids and supraproportional oxygen consumption makes neuronal tissues easily damaged by ionizing radiation [60], and eventually leading to the radiation encephalopathy. Within the brain, hippocampus located in the ventromedial part of the temporal lobes is exceptionally susceptible to a wide variety of toxic insults [61,62]. Hence there is a demand for reliable investigation and apprehension of the effective protection of the normal brain against high-LET carbon ion radiation.

The impact of cognitive impairment in the primary and metastatic brain tumor patient's quality of life is recognized as second only to survival in clinical trials [63,64]. Our present results displayed that the massive cognitive impairment caused by high-LET carbon ion irradiation, as illustrated by their increased latencies to find the hidden platform from the Morris water maze test. This indicates that carbon ions worsened spatial learning and memory abilities. Comparable outcomes from cognition testing were found in the animals, exposing to high-LET ^{56}Fe, ^{28}Si and ^{16}O particle irradiation, even at lower doses [65–67].

With respect to the histopathology evaluation, high-LET carbon ions led to the injured neuron in the brain hippocampus characterized by the Nissl-stained dark neurons, especially in the edge of the DG and CA1 region. The edge of the DG consists of the granule cell layer (GCL) which is critical to the spatial memory formation and the subgranular zone (SGZ) which is one of neurogenic regions in adulthood to correlate with certain aspects of brain cognitive function, including learning and memory [68,69]. Likewise, CA1 region plays a vital role in spatial learning and participating in temporal information of visible objects [70]. These data suggest that carbon-ion induced cognitive changes were mainly manifested as hippocampus-mediated learning and memory deficits.

Cognitive decline is a manifestation of mitochondrial disorders [71] and mitochondrial abnormalities are well-known to cause cognitive impairments as well [72,73]. Our data exhibited that high-LET carbon ions resulted in the swelling of the mitochondria, and impairing mitochondrial dysfunction marked by the reduced activities of tricarboxylic acid cycle enzymes such as PDH, CS, SDH and α-KGDH as

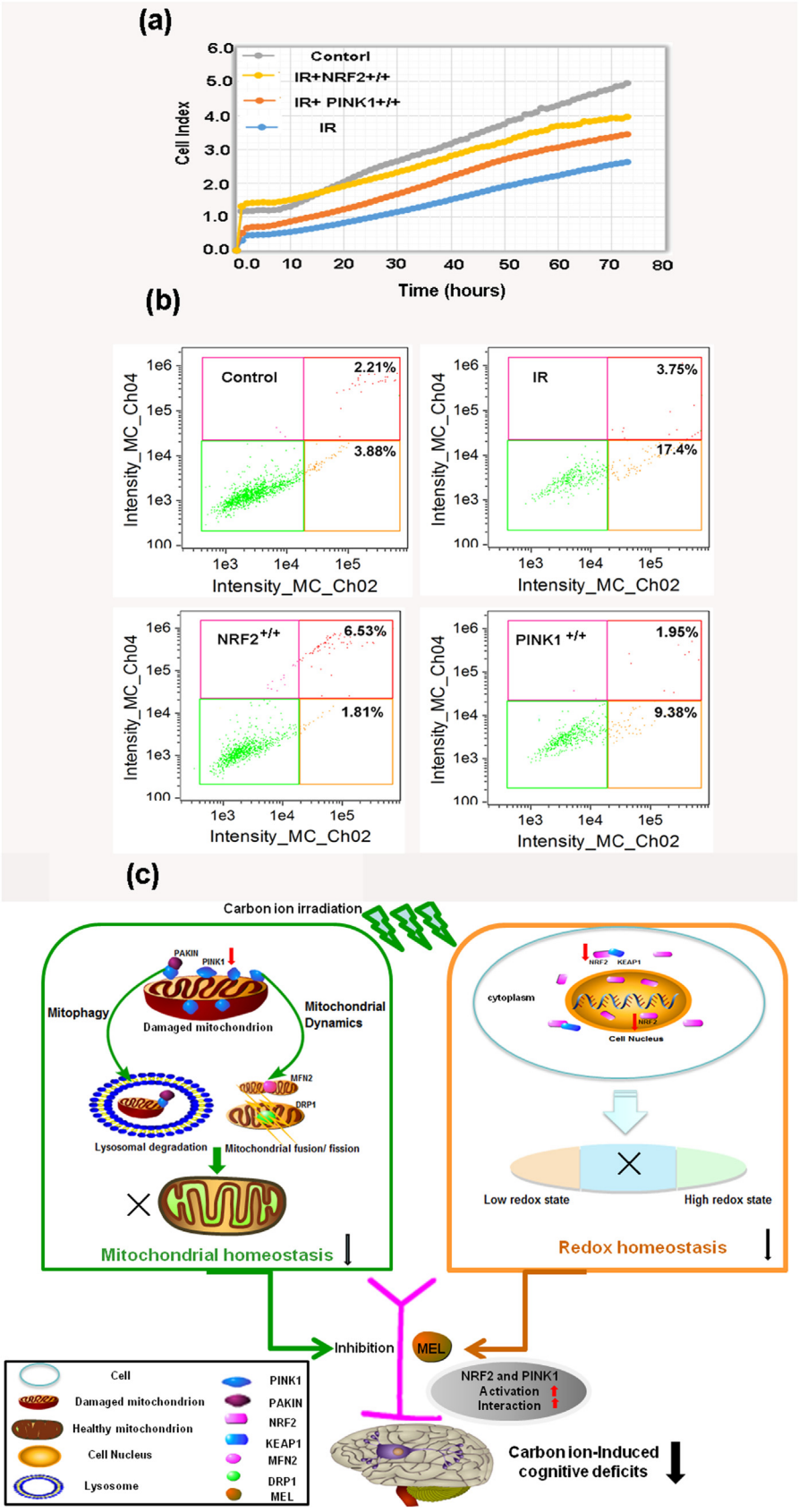

Fig. 8. Lentiviral vector-mediated NRF2 and PINK1 expression modulated the hippocampal cell proliferation and apoptosis. (a) Cell index values were determined every 1 h using an iCELLigence RTCA system for up to 72 h. (b) Annexin V-FITC/PI staining and flow cytometric determination of apoptosis in the cells. Percentage denotes proportion of apoptotic cells in right lower quadrant and right upper quadrant. (c) The proposed mechanisms for the counteraction of cognitive deficits in the mouse model of high-LET carbon ion irradiation.

well as the decreased activities of respiratory chain complexes such as complex I, IV and V. Abnormal mitochondrial morphology and mitochondrial dysfunctions have been reported to disrupt energy metabolism, increase mitochondrial oxidative stress, induce apoptosis, and cause cognitive decline/neurodegenerative disorders [74–76]. Our study also found that carbon ions created a major energy crisis, as reflected by the low ATP yield and the alterations in bioenergetic-related protein abundance from proteomics analysis.

Melatonin as a mitochondria-targeted antioxidant has been documented to accumulate in mitochondria with high concentration, and thus involves in situ in mitochondrial activities and physiology [26,77]. To better understand the mechanism of improvement of carbon ion induced-cognitive deficits, melatonin as a stabilizer of mitochondrial function was pretreated with the carbon ion irradiated animals. In the present study, mitochondrial dynamics and mitophagy as two critical processes underlying mitochondrial homeostasis were investigated.

Our evidence from the identification of mitochondria dynamics-related proteins exhibited that carbon ions reduced the mitofusin-2 (Mfn-2) level, which is a mitochondrial membrane protein that participates in mitochondrial fusion in the mammalian cells. On the other hand, carbon ions elevated the dynamin-related protein 1 (Drp1) level, which is a dynamin-related protein that promotes mitochondrial fission. However, application of melatonin significantly reversed the reduction of Mfn-2 level and the elevation of Drp1 level, which is similar in the cortical neurons after melatonin and 1-methyl-4-phenylpyridinium co-treatment [78].

Compared with the sham-irradiated mice, the animals exposed to carbon ions profoundly dampened the mitophagy, as demonstrated by the decreasing amount of LC3II in mitochondria. However, pretreatment with melatonin effectively reversed the loss of mitophagic progression marked by the significant increase of LC3II level and obvious co-location of LC3 and COX IV. Very recently, several lines of evidence also demonstrate that melatonin promoted mitophagy and improved homeostasis of mitochondria to offer neuroprotection [37,38,79]. Collectively, our data indicated that mitochondrion-targeted antioxidant could modulate mitochondrial dynamics and mitophagy to sustain the mitochondria homeostasis in the carbon ion-irradiated mice.

Oxidative stress is inseparably linked to mitochondrial dysfunction and has been implicated in the cognitive impairment [80–82]. The current study showed the carbon ions induced the persistent oxidative lesions to lipids and DNA, as well as the decreased total antioxidant capacity and mitochondrial antioxidant SOD2. But melatonin effectively eliminated the sustained oxidative injury elicited by high-LET carbon ions. To date, there is a keen interest in the introduction and development of antioxidant therapies for the treatment of cognitive decline. This was further supported by clinical observations of the attenuated oxidative lesions to deplete the mild cognitive impairment and Alzheimer's disease [83].

To further confirm the detail mechanism underlying the effects of carbon ion on the mitochondria homeostasis, we determined the alteration of PINK1-dependent pathway in the presence or absence of melatonin. In mammalian cells, PINK1 and Parkin are critically involved in cell survival and excessive neurological disorders [84,85]. In this study, we demonstrated that PINK1 expression and stabilization at the outer mitochondrial membranes were significantly decreased, especially in the DG region of the hippocampus, accompanied with the down-regulation of PINK1 and Parkin expressions. Deficiency for PINK1 or Parkin could disrupt the damaged mitochondrial degradation and thereby increase oxidative stress due to the accumulation of dysfunctional mitochondria that release ROS [16]. However, in this study, melatonin dramatically reversed the up-regulation of PINK1 and Pakin expression and promoted PINK1 to be stabilized at the mitochondria, and subsequently maintained the mitochondria homeostasis.

The transcription factor NRF2, a master redox switch in turning on the cellular signaling, represents an attractive therapeutic target for neurologic disorders [86]. NRF2 is negatively regulated by the cytoplasmic redox-sensor protein Keap1 via its Neh2 (Nrf2/ECH homology 2) domain [23]. In the current study, we found that NRF2 expression and translocation to the nucleus significantly reduced in the mice subjected to carbon ion exposure while melatonin pretreatment could effectively promote these decreases. Similar results of melatonin received the support of the glioma cells [87] and neural stem cells [88]. As we known, NRF2 as a regulator of oxidative stress also exerts neuroprotective roles in prevention of cognitive impairment [89]. Recently, the emerging role of NRF2 in mitochondrial function has been found, contributing to the overall mitochondrial homeostasis via affecting mitochondrial membrane potential and respiration, oxidative phosphorylation and the synthesis of ATP, mitochondrial biogenesis and mitochondrial integrity [24,25,90].

To better understand whether the relationship exists between NRF2 and PINK1 as two critical neuroprotective proteins, a mutual interplay between NRF2 and PINK1 was detected in the irradiated hippocampus with melatonin pretreatment. We found that melatonin administration facilitated the positive interaction between NRF2 and PINK1 signaling, as evidenced by results from Co-IP and SPR assay. Several lines of evidence also indicate that PINK1 expression could be positively regulated by NRF2 activity and the NRF2/PINK1 signaling axis is closely associated with cell survival and longevity [91–93].

To get detail information about the signaling pathways of the neuroprotection against carbon ions, NRF2 and PINK1 were overexpressed in the mouse hippocampus HT22 cells. HT22 hippocampal cell line, which lacks a functional glutamate receptor, is valuable for studying the molecular mechanism of spatial memory deficits [94,95]. Our study showed that overexpressions NRF2 and PINK1 significantly promoted the cell growth and attenuated the apoptotic populations in $NRF2^{+/+}$ and $PINK1^{+/+}$ hippocampal cells treated with carbon ions, suggesting that NRF2 and PINK1 overexpressing were more resistant to neurotoxins elicited by carbon ion exposure. Consistent with the data of melatonin pretreatment, this demonstrated the major contributions of NRF2 and PINK1 in counteracting carbon-ion induced damage.

Taking these data together, as shown in Fig. 8c, this study illustrated that carbon ion irradiation at 4 Gy induced the obvious spatial cognitive impairments, and disrupted the mitochondrial homeostasis and redox balanced, which closely associated with inactivation of NRF2 and PINK1 signaling. However, administration of melatonin upregulated the NRF2-PINK1 signaling and enhanced the crosstalk between NRF2 and PINK1. Moreover, in $NRF2^{+/+}$ and $PINK1^{+/+}$ hippocampal neuronal cells, the carbon ion-induced reductions in cell proliferation and survival were stirringly ameliorated. As a result, a carbon ion-caused cognitive deficit was effectively reversed through restoring the mitochondrial functions as well as eradicating the oxidative insults.

Acknowledgments

This work was supported by grants from the National Key Projects of Research and Development (2016YFC0904600), Key Program of National Natural Science Foundation of China (U1432248), National Natural Science Foundation of China (No.11575262 and No.11675234). We express our thanks to the accelerator crew at the HIRFL, National Laboratory of Heavy Ion Accelerator in Lanzhou.

Appendix A. Supporting information

Supplementary data associated with this article can be found in the online version at http://dx.doi.org/10.1016/j.redox.2018.04.012.

References

[1] P. Haigron, J.L. Dillenseger, L. Luo, J.L. Coatrieux, Image-guided therapy: evolution and breakthrough, IEEE Eng. Med. Biol. Mag. 29 (2010) 100–104.
[2] A.H. Bhat, K.B. Dar, S. Anees, M.A. Zargar, A. Masood, M.A. Sofi, S.A. Ganie, Oxidative stress, mitochondrial dysfunction and neurodegenerative diseases; a

mechanistic insight, Biomed. Pharmacother. 74 (2015) 101–110.
[3] C. Guo, L. Sun, X. Chen, D. Zhang, Oxidative stress, mitochondrial damage and neurodegenerative diseases, Neural Regen. Res. 8 (2013) 2003–2014.
[4] M. Ruiz, M. Begou, N. Launay, P. Ranea-Robles, Oxidative stress and mitochondrial dynamics malfunction are linked in Pelizaeus-Merzbacher disease, Brain Pathol. (2017), http://dx.doi.org/10.1111/bpa.12571.
[5] M. Picard, B.S. McEwen, Mitochondria impact brain function and cognition, Proc. Natl. Acad. Sci. USA 111 (2014) 7–8.
[6] M. Khacho, A. Clark, D.S. Svoboda, J.G. MacLaurin, D.C. Lagace, D.S. Park, R.S. Slack, Mitochondrial dysfunction underlies cognitive defects as a result of neural stem cell depletion and impaired neurogenesis, Hum. Mol. Genet. 26 (2017) 3327–3341.
[7] X. Zhou, N. Li, Y. Wang, Y. Wang, X. Zhang, H. Zhang, Effects of X-irradiation on mitochondrial DNA damage and its supercoiling formation change, Mitochondrion 11 (2011) 886–892.
[8] X. Zhou, X. Liu, X. Zhang, R. Zhou, Y. He, Q. Li, Z. Wang, H. Zhang, Non-randomized mtDNA damage after ionizing radiation via charge transport, Sci. Rep. 2 (2012) 780.
[9] H. Cui, Y. Kong, H. Zhang, Oxidative stress, mitochondrial dysfunction, and aging, J. Signal Transduct. 2012 (2012) 646354.
[10] C. Sun, Z. Wang, Y. Liu, Y. Liu, H. Li, C. Di, Z. Wu, L. Gan, H. Zhang, Carbon ion beams induce hepatoma cell death by NADPH oxidase-mediated mitochondrial damage, J. Cell. Physiol. 229 (2014) 100–107.
[11] A. Petit, T. Kawarai, E. Paitel, N. Sanjo, M. Maj, M. Scheid, F. Chen, Y. Gu, H. Hasegawa, S. Salehi-Rad, L. Wang, E. Rogaeva, P. Fraser, B. Robinson, P. St George-Hyslop, A. Tandon, Wild-type PINK1 prevents basal and induced neuronal apoptosis, a protective effect abrogated by Parkinson disease-related mutations, J. Biol. Chem. 280 (2005) 34025–34032.
[12] T.G. McWilliams, M.M. Muqit, PINK1 and Parkin: emerging themes in mitochondrial homeostasis, Curr. Opin. Cell Biol. 45 (2017) 83–91.
[13] G. Arena, V. Gelmetti, L. Torosantucci, D. Vignone, G. Lamorte, P. De Rosa, E. Cilia, E.A. Jonas, E.M. Valente, PINK1 protects against cell death induced by mitochondrial depolarization, by phosphorylating Bcl-xL and impairing its pro-apoptotic cleavage, Cell Death Differ. 20 (2013) 920–930.
[14] F. Mouton-Liger, M. Jacoupy, J.C. Corvol, O. Corti, PINK1/Parkin-dependent mitochondrial surveillance: from pleiotropy to Parkinson's disease, Front. Mol. Neurosci. 10 (2017) 120.
[15] C. Rub, A. Wilkening, W. Voos, Mitochondrial quality control by the Pink1/Parkin system, Cell Tissue Res. 367 (2017) 111–123.
[16] S.K. Barodia, R.B. Creed, M.S. Goldberg, Parkin and PINK1 functions in oxidative stress and neurodegeneration, Brain Res. Bull. 133 (2017) 51–59.
[17] J.W. Pridgeon, J.A. Olzmann, L.S. Chin, L. Li, PINK1 protects against oxidative stress by phosphorylating mitochondrial chaperone TRAP1, PLoS Biol. 5 (2007) e172.
[18] C. Henchcliffe, M.F. Beal, Mitochondrial biology and oxidative stress in Parkinson disease pathogenesis, Nat. Clin. Pract. Neurol. 4 (2008) 600–609.
[19] C.A. Gautier, T. Kitada, J. Shen, Loss of PINK1 causes mitochondrial functional defects and increased sensitivity to oxidative stress, Proc. Natl. Acad. Sci. USA 105 (2008) 11364–11369.
[20] S. Torres-Odio, J. Key, H.H. Hoepken, J. Canet-Pons, L. Valek, B. Roller, M. Walter, B. Morales-Gordo, D. Meierhofer, P.N. Harter, M. Mittelbronn, I. Tegeder, S. Gispert, G. Auburger, Progression of pathology in PINK1-deficient mouse brain from splicing via ubiquitination, ER stress, and mitophagy changes to neuroinflammation, J. Neuroinflamm. 14 (2017) 154.
[21] L.E. Otterbein, A.M. Choi, The saga of leucine zippers continues: in response to oxidative stress, Am. J. Respir. Cell Mol. Biol. 26 (2002) 161–163.
[22] S. Sajadimajd, M. Khazaei, Oxidative stress and cancer: the role of Nrf2, Curr. Cancer Drug Targets (2017), http://dx.doi.org/10.2174/1568009617666171002144228.
[23] Q. Ma, Role of nrf2 in oxidative stress and toxicity, Annu. Rev. Pharmacol. Toxicol. 53 (2013) 401–426.
[24] K.M. Holmstrom, R.V. Kostov, A.T. Dinkova-Kostova, The multifaceted role of Nrf2 in mitochondrial function, Curr. Opin. Toxicol. 1 (2016) 80–91.
[25] A.T. Dinkova-Kostova, A.Y. Abramov, The emerging role of Nrf2 in mitochondrial function, Free Radic. Biol. Med. 88 (2015) 179–188.
[26] D.X. Tan, L.C. Manchester, L. Qin, R.J. Reiter, Melatonin: a mitochondrial targeting molecule involving mitochondrial protection and dynamics, Int. J. Mol. Sci. 17 (2016).
[27] S.A. Rosales-Corral, D. Acuna-Castroviejo, A. Coto-Montes, J.A. Boga, L.C. Manchester, L. Fuentes-Broto, A. Korkmaz, S. Ma, D.X. Tan, R.J. Reiter, Alzheimer's disease: pathological mechanisms and the beneficial role of melatonin, J. Pineal Res. 52 (2012) 167–202.
[28] A. Naskar, V. Prabhakar, R. Singh, D. Dutta, K.P. Mohanakumar, Melatonin enhances L-DOPA therapeutic effects, helps to reduce its dose, and protects dopaminergic neurons in 1-methyl-4-phenyl-1,2,3,6-tetrahydropyridine-induced Parkinsonism in mice, J. Pineal Res. 58 (2015) 262–274.
[29] R. Hardeland, Melatonin and the theories of aging: a critical appraisal of melatonin's role in antiaging mechanisms, J. Pineal Res. 55 (2013) 325–356.
[30] A. Agorastos, A.C. Linthorst, Potential pleiotropic beneficial effects of adjuvant melatonergic treatment in posttraumatic stress disorder, J. Pineal Res. 61 (2016) 3–26.
[31] Y. Yang, S. Jiang, Y. Dong, C. Fan, L. Zhao, X. Yang, J. Li, S. Di, L. Yue, G. Liang, R.J. Reiter, Y. Qu, Melatonin prevents cell death and mitochondrial dysfunction via a SIRT1-dependent mechanism during ischemic-stroke in mice, J. Pineal Res. 58 (2015) 61–70.
[32] S. Liu, Y. Guo, Q. Yuan, Y. Pan, L. Wang, Q. Liu, F. Wang, J. Wang, A. Hao, Melatonin prevents neural tube defects in the offspring of diabetic pregnancy, J. Pineal Res. 59 (2015) 508–517.
[33] J. Chen, G. Chen, J. Li, C. Qian, H. Mo, C. Gu, F. Yan, W. Yan, L. Wang, Melatonin attenuates inflammatory response-induced brain edema in early brain injury following a subarachnoid hemorrhage: a possible role for the regulation of pro-inflammatory cytokines, J. Pineal Res. 57 (2014) 340–347.
[34] R. Sharafati-Chaleshtori, H. Shirzad, M. Rafieian-Kopaei, A. Soltani, Melatonin and human mitochondrial diseases, J. Res. Med. Sci. 22 (2017) 2.
[35] E. Parada, I. Buendia, R. Leon, P. Negredo, A. Romero, A. Cuadrado, M.G. Lopez, J. Egea, Neuroprotective effect of melatonin against ischemia is partially mediated by alpha-7 nicotinic receptor modulation and HO-1 overexpression, J. Pineal Res. 56 (2014) 204–212.
[36] Z. Wang, C. Ma, C.J. Meng, G.Q. Zhu, X.B. Sun, L. Huo, J. Zhang, H.X. Liu, W.C. He, X.M. Shen, Z. Shu, G. Chen, Melatonin activates the Nrf2-ARE pathway when it protects against early brain injury in a subarachnoid hemorrhage model, J. Pineal Res. 53 (2012) 129–137.
[37] X. Onphachanh, H.J. Lee, J.R. Lim, Y.H. Jung, J.S. Kim, C.W. Chae, S.J. Lee, A.A. Gabr, H.J. Han, Enhancement of high glucose-induced PINK1 expression by melatonin stimulates neuronal cell survival: Involvement of MT2 /Akt/NF-kappaB pathway, J. Pineal Res. 63 (2017).
[38] M.E. Diaz-Casado, E. Lima, J.A. Garcia, C. Doerrier, P. Aranda, R.K. Sayed, A. Guerra-Librero, G. Escames, L.C. Lopez, D. Acuna-Castroviejo, Melatonin rescues zebrafish embryos from the parkinsonian phenotype restoring the parkin/PINK1/DJ-1/MUL1 network, J. Pineal Res. 61 (2016) 96–107.
[39] X. Chen, A. Hao, X. Li, Z. Du, H. Li, H. Wang, H. Yang, Z. Fang, Melatonin inhibits tumorigenicity of glioblastoma stem-like cells via the AKT-EZH2-STAT3 signaling axis, J. Pineal Res. 61 (2016) 208–217.
[40] X. Zheng, B. Pang, G. Gu, T. Gao, R. Zhang, Q. Pang, Q. Liu, Melatonin inhibits glioblastoma stem-like cells through suppression of EZH2-NOTCH1 signaling axis, Int. J. Biol. Sci. 13 (2017) 245–253.
[41] R.M. Sainz, J.C. Mayo, C. Rodriguez, D.X. Tan, S. Lopez-Burillo, R.J. Reiter, Melatonin and cell death: differential actions on apoptosis in normal and cancer cells, Cell. Mol. Life Sci. 60 (2003) 1407–1426.
[42] R.J. Reiter, J.C. Mayo, D.X. Tan, R.M. Sainz, M. Alatorre-Jimenez, L. Qin, Melatonin as an antioxidant: under promises but over delivers, J. Pineal Res. 61 (2016) 253–278.
[43] R.J. Reiter, S.A. Rosales-Corral, D.X. Tan, D. Acuna-Castroviejo, L. Qin, S.F. Yang, K. Xu, Melatonin, a full service anti-cancer agent: inhibition of initiation, progression and metastasis, Int. J. Mol. Sci. 18 (2017).
[44] M.R. Vianna, M. Alonso, H. Viola, J. Quevedo, F. de Paris, M. Furman, M.L. de Stein, J.H. Medina, I. Izquierdo, Role of hippocampal signaling pathways in long-term memory formation of a nonassociative learning task in the rat, Learn. Mem. 7 (2000) 333–340.
[45] K. Chiu, W.M. Lau, H.T. Lau, K.F. So, R.C. Chang, Micro-dissection of rat brain for RNA or protein extraction from specific brain region, J. Vis. Exp. (2007) 269.
[46] K. Bromley-Brits, Y. Deng, W. Song, Morris water maze test for learning and memory deficits in Alzheimer's disease model mice, J. Vis. Exp. (2011).
[47] C. Sun, X. Liu, C. Di, Z. Wang, X. Mi, Y. Liu, Q. Zhao, A. Mao, W. Chen, L. Gan, H. Zhang, MitoQ regulates autophagy by inducing a pseudo-mitochondrial membrane potential, Autophagy 13 (2017) 730–738.
[48] Y. Wang, Q. Hou, G. Xiao, S. Yang, C. Di, J. Si, R. Zhou, Y. Ye, Y. Zhang, H. Zhang, Selective ATP hydrolysis inhibition in F1Fo ATP synthase enhances radiosensitivity in non-small-cell lung cancer cells (A549), Oncotarget 8 (2017) 53602–53612.
[49] G. Liu, Y. Wang, G.J. Anderson, C. Camaschella, Y. Chang, G. Nie, Functional analysis of GLRX5 mutants reveals distinct functionalities of GLRX5 protein, J. Cell. Biochem. 117 (2016) 207–217.
[50] Y.L. Yang, J. Li, K. Liu, L. Zhang, Q. Liu, B. Liu, L.W. Qi, Ginsenoside Rg5 increases cardiomyocyte resistance to ischemic injury through regulation of mitochondrial hexokinase-II and dynamin-related protein 1, Cell Death Dis. 8 (2017) e2625.
[51] S. Lin, A. Ren, L. Wang, Y. Huang, Y. Wang, C. Wang, N. Greene, Oxidative stress and apoptosis in Benzo[a]pyrene-induced neural tube defects, Free Radic. Biol. Med. 116 (2018) 149–158.
[52] L. Zhang, J. Yan, Y. Liu, Q. Zhao, C. Di, S. Chao, L. Jie, Y. Liu, H. Zhang, Contribution of caspase-independent pathway to apoptosis in malignant glioma induced by carbon ion beams, Oncol. Rep. 37 (2017) 2994–3000.
[53] R. Limame, A. Wouters, B. Pauwels, E. Fransen, M. Peeters, F. Lardon, O. De Wever, P. Pauwels, Comparative analysis of dynamic cell viability, migration and invasion assessments by novel real-time technology and classic endpoint assays, PLoS One 7 (2012) e46536.
[54] P.K. Pilly, S. Grossberg, How do spatial learning and memory occur in the brain? Coordinated learning of entorhinal grid cells and hippocampal place cells, J. Cogn. Neurosci. 24 (2012) 1031–1054.
[55] P. Vigie, N. Camougrand, [Role of mitophagy in the mitochondrial quality control], Med. Sci. 33 (2017) 231–237.
[56] E.E. Vomhof-Dekrey, M.J. Picklo Sr., The Nrf2-antioxidant response element pathway: a target for regulating energy metabolism, J. Nutr. Biochem. 23 (2012) 1201–1206.
[57] D.K. Ebner, T. Kamada, The emerging role of carbon-ion radiotherapy, Front. Oncol. 6 (2016) 140.
[58] H. Zhang, S. Li, X.H. Wang, Q. Li, S.H. Wei, L.Y. Gao, W.P. Zhao, Z.G. Hu, R.S. Mao, H.S. Xu, Q.N. Zhang, Y.J. Yue, Z.Z. Tian, J.T. Ran, G.Q. Xiao, W.L. Zhan, Results of carbon ion radiotherapy for skin carcinomas in 45 patients, Br. J. Dermatol. 166 (2012) 1100–1106.
[59] R. Pathak, S.K. Dey, A. Sarma, A.R. Khuda-Bukhsh, Cell killing, nuclear damage and apoptosis in Chinese hamster V79 cells after irradiation with heavy-ion beams of (16)O, (12)C and (7)Li, Mutat. Res. 632 (2007) 58–68.

[60] M. Karbownik, R.J. Reiter, Antioxidative effects of melatonin in protection against cellular damage caused by ionizing radiation, Proc. Soc. Exp. Biol. Med. 225 (2000) 9–22.
[61] A.L. McCormack, M. Thiruchelvam, A.B. Manning-Bog, C. Thiffault, J.W. Langston, D.A. Cory-Slechta, D.A. Di Monte, Environmental risk factors and Parkinson's disease: selective degeneration of nigral dopaminergic neurons caused by the herbicide paraquat, Neurobiol. Dis. 10 (2002) 119–127.
[62] R. Rao, M. de Ungria, D. Sullivan, P. Wu, J.D. Wobken, C.A. Nelson, M.K. Georgieff, Perinatal brain iron deficiency increases the vulnerability of rat hippocampus to hypoxic ischemic insult, J. Nutr. 129 (1999) 199–206.
[63] S. Balentova, M. Adamkov, Molecular, cellular and functional effects of radiation-induced brain injury: a review, Int. J. Mol. Sci. 16 (2015) 27796–27815.
[64] M.T. Makale, C.R. McDonald, J.A. Hattangadi-Gluth, S. Kesari, Mechanisms of radiotherapy-associated cognitive disability in patients with brain tumours, Nat. Rev. Neurol. 13 (2017) 52–64.
[65] M.A. Suresh Kumar, M. Peluso, P. Chaudhary, J. Dhawan, A. Beheshti, K. Manickam, U. Thapar, L. Pena, M. Natarajan, L. Hlatky, B. Demple, M. Naidu, Fractionated radiation exposure of rat spinal cords leads to latent neuro-inflammation in brain, cognitive deficits, and alterations in apurinic endonuclease 1, PLoS One 10 (2015) e0133016.
[66] J. Yan, Y. Liu, Q. Zhao, J. Li, A. Mao, H. Li, C. Di, H. Zhang, 56 Fe irradiation-induced cognitive deficits through oxidative stress in mice, Toxicol. Res. 5 (2016) 1672–1679.
[67] S.M. Poulose, D.F. Bielinski, K. Carrihill-Knoll, B.M. Rabin, B. Shukitt-Hale, Exposure to 16O-particle radiation causes aging-like decrements in rats through increased oxidative stress, inflammation and loss of autophagy, Radiat. Res. 176 (2011) 761–769.
[68] R.E. Clark, N.J. Broadbent, L.R. Squire, Hippocampus and remote spatial memory in rats, Hippocampus 15 (2005) 260–272.
[69] C.D. Mandyam, The interplay between the hippocampus and amygdala in regulating aberrant hippocampal neurogenesis during protracted abstinence from alcohol dependence, Front. Psychiatry 4 (2013) 61.
[70] J. Hoge, R.P. Kesner, Role of CA3 and CA1 subregions of the dorsal hippocampus on temporal processing of objects, Neurobiol. Learn. Mem. 88 (2007) 225–231.
[71] J. Finsterer, Cognitive decline as a manifestation of mitochondrial disorders (mitochondrial dementia), J. Neurol. Sci. 272 (2008) 20–33.
[72] N. Lomeli, K. Di, J. Czerniawski, J.F. Guzowski, D.A. Bota, Cisplatin-induced mitochondrial dysfunction is associated with impaired cognitive function in rats, Free Radic. Biol. Med. 102 (2017) 274–286.
[73] S. Yan, F. Du, L. Wu, Z. Zhang, C. Zhong, Q. Yu, Y. Wang, L.F. Lue, D.G. Walker, J.T. Douglas, S.S. Yan, F1F0 ATP synthase-cyclophilin D interaction contributes to diabetes-induced synaptic dysfunction and cognitive decline, Diabetes 65 (2016) 3482–3494.
[74] W.W. Kam, R.B. Banati, Effects of ionizing radiation on mitochondria, Free Radic. Biol. Med. 65 (2013) 607–619.
[75] V.A. Morais, B. De Strooper, Mitochondria dysfunction and neurodegenerative disorders: cause or consequence, J. Alzheimer's Dis. 20 (Suppl 2) (2010) S255–S263.
[76] T.G. Demarest, M.M. McCarthy, Sex differences in mitochondrial (dys)function: implications for neuroprotection, J. Bioenerg. Biomembr. 47 (2015) 173–188.
[77] G. Paradies, G. Petrosillo, V. Paradies, R.J. Reiter, F.M. Ruggiero, Melatonin, cardiolipin and mitochondrial bioenergetics in health and disease, J. Pineal Res. 48 (2010) 297–310.
[78] J.I. Chuang, I.L. Pan, C.Y. Hsieh, C.Y. Huang, P.C. Chen, J.W. Shin, Melatonin prevents the dynamin-related protein 1-dependent mitochondrial fission and oxidative insult in the cortical neurons after 1-methyl-4-phenylpyridinium treatment, J. Pineal Res. 61 (2016) 230–240.
[79] S. Cao, S. Shrestha, J. Li, X. Yu, J. Chen, F. Yan, G. Ying, C. Gu, L. Wang, G. Chen, Melatonin-mediated mitophagy protects against early brain injury after subarachnoid hemorrhage through inhibition of NLRP3 inflammasome activation, Sci. Rep. 7 (2017) 2417.
[80] J. Lee, S. Giordano, J. Zhang, Autophagy, mitochondria and oxidative stress: cross-talk and redox signalling, Biochem. J. 441 (2012) 523–540.
[81] G.C. Kujoth, A. Hiona, T.D. Pugh, S. Someya, K. Panzer, S.E. Wohlgemuth, T. Hofer, A.Y. Seo, R. Sullivan, W.A. Jobling, J.D. Morrow, H. Van Remmen, J.M. Sedivy, T. Yamasoba, M. Tanokura, R. Weindruch, C. Leeuwenburgh, T.A. Prolla, Mitochondrial DNA mutations, oxidative stress, and apoptosis in mammalian aging, Science 309 (2005) 481–484.
[82] R. Liu, I.Y. Liu, X. Bi, R.F. Thompson, S.R. Doctrow, B. Malfroy, M. Baudry, Reversal of age-related learning deficits and brain oxidative stress in mice with superoxide dismutase/catalase mimetics, Proc. Natl. Acad. Sci. USA 100 (2003) 8526–8531.
[83] M.C. Polidori, G. Nelles, Antioxidant clinical trials in mild cognitive impairment and Alzheimer's disease - challenges and perspectives, Curr. Pharm. Des. 20 (2014) 3083–3092.
[84] E.M. Valente, P.M. Abou-Sleiman, V. Caputo, M.M. Muqit, K. Harvey, S. Gispert, Z. Ali, D. Del Turco, A.R. Bentivoglio, D.G. Healy, A. Albanese, R. Nussbaum, R. Gonzalez-Maldonado, T. Deller, S. Salvi, P. Cortelli, W.P. Gilks, D.S. Latchman, R.J. Harvey, B. Dallapiccola, G. Auburger, N.W. Wood, Hereditary early-onset Parkinson's disease caused by mutations in PINK1, Science 304 (2004) 1158–1160.
[85] P.H. Reddy, Role of mitochondria in neurodegenerative diseases: mitochondria as a therapeutic target in Alzheimer's disease, CNS Spectr. 14 (2009) 8–13 (discussion16-18).
[86] E.E. Benarroch, Nrf2, cellular redox regulation, and neurologic implications, Neurology 88 (2017) 1942–1950.
[87] P. Jumnongprakhon, P. Govitrapong, C. Tocharus, D. Pinkaew, J. Tocharus, Melatonin protects methamphetamine-induced neuroinflammation through NF-kappaB and Nrf2 pathways in glioma cell line, Neurochem. Res. 40 (2015) 1448–1456.
[88] J. Song, S.M. Kang, K.M. Lee, J.E. Lee, The protective effect of melatonin on neural stem cell against LPS-induced inflammation, Biomed. Res. Int. 2015 (2015) 854359.
[89] C. Branca, E. Ferreira, T.V. Nguyen, K. Doyle, A. Caccamo, S. Oddo, Genetic reduction of Nrf2 exacerbates cognitive deficits in a mouse model of Alzheimer's disease, Hum. Mol. Genet. 26 (2017) 4823–4835.
[90] K. Itoh, P. Ye, T. Matsumiya, K. Tanji, T. Ozaki, Emerging functional cross-talk between the Keap1-Nrf2 system and mitochondria, J. Clin. Biochem. Nutr. 56 (2015) 91–97.
[91] L. Xiao, X. Xu, F. Zhang, M. Wang, Y. Xu, D. Tang, J. Wang, Y. Qin, Y. Liu, C. Tang, L. He, A. Greka, Z. Zhou, F. Liu, Z. Dong, L. Sun, The mitochondria-targeted antioxidant MitoQ ameliorated tubular injury mediated by mitophagy in diabetic kidney disease via Nrf2/PINK1, Redox Biol. 11 (2017) 297–311.
[92] H. Murata, H. Takamatsu, S. Liu, K. Kataoka, N.H. Huh, M. Sakaguchi, NRF2 regulates PINK1 expression under oxidative stress conditions, PLoS One 10 (2015) e0142438.
[93] Y. Kitagishi, N. Nakano, M. Ogino, M. Ichimura, A. Minami, S. Matsuda, PINK1 signaling in mitochondrial homeostasis and in aging (Review), Int. J. Mol. Med. 39 (2017) 3–8.
[94] S.J. Kempf, S. Buratovic, C. von Toerne, S. Moertl, B. Stenerlow, S.M. Hauck, M.J. Atkinson, P. Eriksson, S. Tapio, Ionising radiation immediately impairs synaptic plasticity-associated cytoskeletal signalling pathways in HT22 cells and in mouse brain: an in vitro/in vivo comparison study, PLoS One 9 (2014) e110464.
[95] S.M. Ahn, Y.R. Kim, H.N. Kim, Y.W. Choi, J.W. Lee, C.M. Kim, J.U. Baek, H.K. Shin, B.T. Choi, Neuroprotection and spatial memory enhancement of four herbal mixture extract in HT22 hippocampal cells and a mouse model of focal cerebral ischemia, BMC Complement. Altern. Med. 15 (2015) 202.